

Embedment Strength of Cross-Laminated Timber for Smooth Dowel-type Fasteners

Wei-qun Dong¹, Qiao Li¹, Hao Zhang¹, Zhi-qiang Wang^{1,*}, Jian-hui Zhou², and Meng Gong³

¹College of Materials Science and Engineering, Nanjing Forestry University, 159 Longpan Road, Nanjing, Jiangsu 210037, China

²Integrated Wood Engineering, University of Northern British Columbia, 499 George St Prince George, BC Canada V2L 1R7

³Wood Science and Technology Centre, University of New Brunswick, 1350 Regent Street, Fredericton, NB E3C 2G6, Canada

Abstract. Embedment strength is a significant property in the dowel type connection in timber structure, i.e. cross-laminated timber (CLT). The CLT design properties are different from those of sawn timber (ST) and glued-laminated timber (GLT) because of the orthogonal structure, which may particularly have influence on the design of connections. The layup feature, i.e. the thickness ratio of transverse layer (TRL) was considered as an effective factor on CLT embedment strength in this study, except for other factors, i.e. wood density, smooth dowel diameter, and loading angle. Approximate 660 embedment tests were performed according to ASTM D5764 half-hole test method. A few of existing design models for CLT embedment strength were evaluated using experimental data. It was found that different factors had different effect tendency and each factor had statistically significant impact on CLT embedment strength. The embedment strength and failure modes of CLT were obviously different from those of GLT due to the existence of transverse layer in CLT. The existing design equations should be improved. Based on the test results, a new design equation was proposed which had better prediction.

1 Introduction

Cross-laminated timber (CLT) is an innovative wood product that was first developed in Austria and Germany in the early 1990s. And it is made of at least three orthogonally bonded layers of solid sawn lumber or structural composite lumber (SCL) using adhesive, nails or wooden dowels [1]. Compared with solid timber (ST) and glued-laminated timber (GLT), CLT has some characteristics in configuration, such as gaps or edge-gluing between lumbers in the same layer, potential stress reliefs in lumber and orthogonal layup of CLT. Previous researches had verified that these characteristics had effects on the physical and mechanical properties of CLT [1-4].

The orthogonal layup makes the connection properties of CLT complicated due to the significant differences of embedment strength, deformation ductility and failure modes between longitudinal and transverse layers. The existence of transverse layers would reduce the embedment strength and improve the failure ductility of CLT under embedment tests [3]. Furthermore, the normal CLT panel has layers oriented perpendicular to each other, however, in special configurations, consecutive layers may be placed in the same direction, giving a double layer (e.g. double longitudinal layers at the outer faces and additional double layers at the core of the panel) to obtain specific structural capacities [5]. The existing design equations for embedment strength of

wood or wood-based panels under dowel-type fasteners may not be valid for CLT [6].

The connection properties play a very important role for the structural properties of CLT construction. About 80% of structural failures have their origin on connection [7]. The yielding resistance of the fastener, the assembly's geometry and the embedment strength of wood are the most important parameters affecting the timber connection design based on European yield model (EYM). Furthermore, embedment strength is not a unique property, but one dependent upon a few of factors, e.g. the relative density of wood, diameter and cross-sectional shape of fastener, loading angle (loading angle relative to the specimen face grain), test method and so on [8,9]. There are two main ways to study CLT embedment property at present. First, based on the effect of dowel diameter, wood density and loading angle on CLT embedment strength, the theoretical calculation models of CLT were developed. Second, combined with CLT characteristics in configuration, e.g. the existence of gaps and transverse layer, the prediction models were also built [1,6,10-13]. Uibel and Blaß were the first to investigate laterally-loaded dowel-type fasteners in CLT plane and narrow sides by means of Central European CLT and solid wood-based panels. Two prediction models based on multiple regression analysis were built, e.g. Equation (3) and (4) presented in 3.3.1. The first model shown in Equation (3) is quite general and is independent of the type of lay-up of the panel, however, the second model shown in Equation (4) is panel build-

* Corresponding author: wangzhiqiang@njfu.edu.cn

up specific. Kennedy et al. carried on approximate 720 Canadian CLT embedment tests with lag screws and self-drilling screws with diameters ranging from 6.0 mm to 19.1 mm. A nonlinear regression model, independent of the panel layup and the fastener diameter, was developed, i.e. Equation (6) and (7) presented in 3.3.2 [6].

In addition, there are different design models for CLT embedment strength adopted by different codes. For example, in the US edition of the CLT Handbook, the CLT embedment strength model is a function of the embedment strength and fastener bearing length of parallel and cross layers and the angle of load to the grain of the face layer, i.e. Equation (8), (9) and (10) presented in 3.3.3. On the other hand, for fasteners installed in the plane face of CLT, only a adjustment factor ($J_k=0.9$), was introduced to CLT when calculating the embedment strength of parallel layer, and then the embedment strength was also calculated based on the Hankinson formula as follows in CSA O86, Equation (11) and (12) presented in 3.3.4 [13].

The purpose of this research is first to investigate the influences of several factors, i.e. fastener diameter, loading angle, wood density and the thickness ratio of transverse layer (TRTL) on CLT embedment strength. Then several existing design models for CLT embedment strength were evaluated by experimental data and a new predictive model was developed finally.

2 Materials and methods

Three wood species or species group, i.e. Spruce-pine-fir (SPF) commercial species group, Douglas fir (*Pseudotsuga menziesii*) and Southern pine (*Pinus taeda*), were used to produce CLT specimens for embedment tests. The used dimension lumbars had thickness 38 mm and width 89 mm with average moisture contents 11-12%. Three-layer CLT test specimens were bonded using one-component polyurethane adhesive (Purbond HB S709). The pressure used was 1.0 MPa, the adhesive coverage was 180 g/m², the pressing time was 3h and the environment temperature varied from 20°C to 25°C during cold pressing. The embedment tests were conducted one month after specimens were fabricated. Table 1 presented the statistic data of specimen density.

Table 1. Density of CLT test specimens

| Wood species | n | ρ_{mean} (kg/m ³) | COV (%) | $\rho_{0.05}$ (kg/m ³) |
|---------------|-----|---------------------------------------|------------|---------------------------------------|
| SPF | 280 | 430 | 4.33 | 400 |
| Southern pine | 140 | 580 | 4.30 | 540 |
| Douglas fir | 240 | 570 | 8.52 | 480 |

Embedment tests were performed using smooth dowels with diameter 10 mm, 12 mm and 14 mm inserted perpendicular to the face of CLT panel and loaded under 0°, 45° or 90° to the grain direction of the outer layer of CLT specimens in this study. Further, the TRTL of CLT was also considered as another important factor having effect on CLT embedment strength. Table 2 shows the arrangement of TRTL. A total of 33 test

groups and approximate 660 test specimens were prepared for embedment tests (20 replications were tested for each group), Table 3. These groups were divided into two classes. The first class, group 1 to 21, having constant TRTL 33%, was set to evaluate the effects of fastener diameter, loading angle, wood density (species) on CLT embedment strength. Then the second class, group 22 to 33, including two wood species or species group (SPF and Douglas fir) and having constant fastener diameter (12 mm), loading angle (0°), was used to determine the influence of TRTL.

Table 2. Thickness ratio of transverse layer of CLT specimens

| Layup | Layer thickness (mm) | TRTL (%) | Production type |
|---------|-------------------------|-------------|--------------------|
| //-// | 20-20-20 | 0 | GLT |
| //-⊥-// | 24-12-24 | 20 | CLT |
| //-⊥-// | 20-20-20 | 33 | CLT |
| //-⊥-// | 18-24-18 | 40 | CLT |
| //-⊥-// | 15-30-15 | 50 | CLT |
| //-⊥-// | 12-36-12 | 60 | CLT |
| ⊥-⊥-⊥ | 20-20-20 | 100 | GLT |

Where, // indicates layer with grain parallel to loading. ⊥ indicates layer with grain perpendicular to loading.

Embedment tests were conducted according to ASTM D5764 half-hole test method in this study as shown in Fig. 1. The test specimen was a 60 mm cube.

The specimens were loaded at a constant speed of 1.0 mm/min and the test was terminated at an embedment of one half the dowel diameter or after maximum load had been reached. The failure modes were recorded and the embedment strength presented the measured stress (f_i) as the 5% diameter offset load (P_y) divided by the embedded length (l) and the nominal diameter (d) of the dowel, Equation (1).

$$f_i = \frac{P_y}{l \cdot d} \quad (1)$$

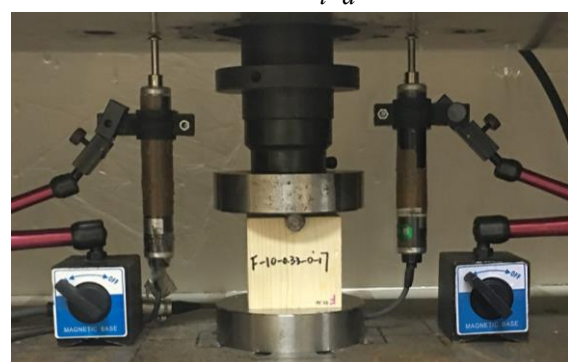


Fig. 1. Embedment test set-up

3 Results and discussion

Table 3 shows the statistic test results of each test group.

Table 3. Results of embedment test

| Group | Specimen notation | Mean (MPa) | Max. (MPa) | Min. (MPa) | COV (%) |
|-------|----------------------|---------------|---------------|---------------|------------|
|-------|----------------------|---------------|---------------|---------------|------------|

| | | | | | |
|----|---------------------------|-------|-------|-------|-------|
| 1 | F-10-0.33-0 ^a | 36.02 | 39.39 | 31.63 | 6.15 |
| 2 | F-10-0.33-90 | 27.14 | 31.92 | 22.90 | 9.35 |
| 3 | F-12-0.33-0 | 30.58 | 34.27 | 27.10 | 6.81 |
| 4 | F-12-0.33-45 | 22.98 | 24.59 | 19.29 | 5.93 |
| 5 | F-12-0.33-90 | 21.69 | 23.61 | 19.80 | 6.06 |
| 6 | F-14-0.33-0 | 25.41 | 27.59 | 22.83 | 5.13 |
| 7 | F-14-0.33-45 | 23.34 | 27.99 | 19.64 | 10.79 |
| 8 | F-14-0.33-90 | 17.85 | 21.50 | 15.79 | 6.67 |
| 9 | N ^b -10-0.33-0 | 50.80 | 56.54 | 46.75 | 4.52 |
| 10 | N-10-0.33-90 | 37.23 | 41.77 | 31.61 | 6.93 |
| 11 | N-12-0.33-0 | 39.60 | 43.50 | 35.26 | 5.60 |
| 12 | N-12-0.33-45 | 37.33 | 44.95 | 28.66 | 14.07 |
| 13 | N-12-0.33-90 | 30.00 | 33.04 | 25.41 | 6.41 |
| 14 | N-14-0.33-0 | 33.97 | 36.28 | 31.16 | 4.19 |
| 15 | N-14-0.33-90 | 25.02 | 28.02 | 22.47 | 6.33 |
| 16 | H ^c -10-0.33-0 | 48.06 | 54.72 | 40.08 | 8.51 |
| 17 | H-10-0.33-90 | 37.32 | 41.86 | 33.80 | 5.66 |
| 18 | H-12-0.33-0 | 38.82 | 42.97 | 34.80 | 6.53 |
| 19 | H-12-0.33-90 | 26.61 | 30.43 | 23.37 | 7.10 |
| 20 | H-14-0.33-0 | 33.87 | 37.87 | 28.75 | 8.77 |
| 21 | H-14-0.33-90 | 23.16 | 26.37 | 20.05 | 6.84 |
| 22 | F-12-0.00-0 | 39.29 | 44.16 | 33.32 | 7.95 |
| 23 | F-12-0.20-0 | 30.63 | 32.67 | 28.15 | 4.46 |
| 24 | F-12-0.40-0 | 26.52 | 28.92 | 23.75 | 5.64 |
| 25 | F-12-0.50-0 | 21.94 | 24.15 | 19.83 | 5.47 |
| 26 | F-12-0.60-0 | 22.90 | 25.00 | 20.63 | 5.26 |
| 27 | F-12-1.00-90 ^d | 14.78 | 17.47 | 11.74 | 10.70 |
| 28 | H-12-0.00-0 | 44.47 | 49.15 | 40.05 | 5.69 |
| 29 | H-12-0.20-0 | 42.92 | 46.70 | 38.34 | 5.72 |
| 30 | H-12-0.40-0 | 35.45 | 38.29 | 32.30 | 5.03 |
| 31 | H-12-0.50-0 | 35.07 | 38.33 | 30.58 | 6.12 |
| 32 | H-12-0.60-0 | 31.71 | 34.59 | 27.81 | 5.44 |
| 33 | H-12-1.00-90 | 17.29 | 18.91 | 15.55 | 5.04 |

Where, F refers to SPF, N refers to Southern pine, H refers to Douglas fir. ^a indicates F specimen, having TRTL 33%, and tested under 0° loading with dowel diameter 10 mm. ^b and ^c indicates the wood species of specimen is Southern pine and Douglas fir, respectively. ^d in order to get TRTL 100%, the loading angel should be 90°.

3.1 Effect of wood density, dowel diameter and loading angle

Fig. 2 shows the average dowel embedment strength of test groups having constant TRTL 33%. It is obvious that different factors, i.e. wood density (species), dowel diameter and loading angle, have different influences on CLT embedment strength. As shown in Table 1, the mean density of SPF CLT is lower than Southern pine CLT and Douglas fir CLT which have similar mean density. Accordingly, the similar tendency was observed about the mean embedment strength. CLT embedment strength increased as wood density increased. Same conclusion had been made in some previous researches

[9,14]. Furthermore, it also could be seen from Fig. 2 that CLT embedment strength decreased as dowel diameter or loading angle increased. The reasons for loading angle effect were that CLT specimens tested under 45° or 90° had most of their layers embedment under 45° or 90° which had lower embedment strength than loaded under 0°. As for the size (diameter) of the fastener, the influence tendency of it is still questionable [8,14].

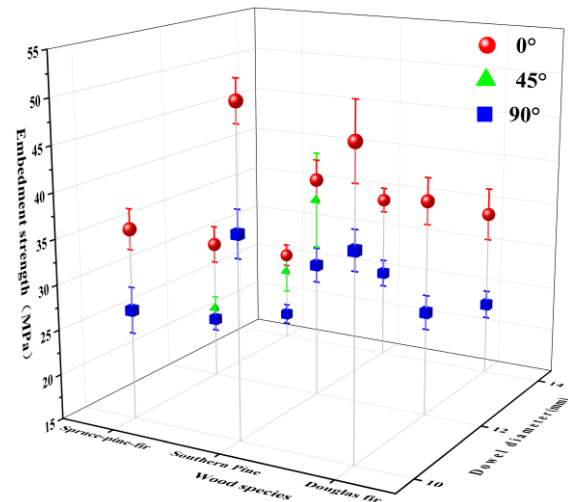


Fig. 2. Effect of wood species(density), dowel diameter and loading angle on CLT embedment strength

In addition, the statistically significant differences of each factor were analyzed in one-way analysis of variance in this study. The results of one-way analysis of variance are summarized in Table 4. It was clear that all of these three factors, i.e. wood density(species), dowel diameter and loading angle, had statistically significant impact on CLT embedment strength except the dowel diameter impact for test specimens with SPF species group and loaded under 45°.

Table 4. Results of one-way analysis of variance

| Wood species | | | |
|---------------------|---------------------|--------------------|-------|
| Dowel diameter (mm) | Loading angle (°) | | |
| | 0 | 45 | 90 |
| 10 | 0.00* ^a | - | 0.00* |
| 12 | 0.00* | 0.00* | 0.00* |
| 14 | 0.00* | - | 0.00* |
| Dowel diameter | | | |
| Wood species | Loading angle (°) | | |
| | 0 | 45 | 90 |
| SPF | 0.00* ^b | 0.604 | 0.00* |
| Southern pine | 0.00* | - | 0.00* |
| Douglas fir | 0.00* | - | 0.00* |
| Loading angle | | | |
| Wood species | Dowel diameter (mm) | | |
| | 10 | 12 | 14 |
| SPF | 0.00* | 0.00* | 0.00* |
| Southern pine | 0.00* | 0.00* ^c | 0.00* |
| Douglas fir | 0.00* | 0.00* | 0.00* |

Where, * indicates a significant difference when the P-value is less than 0.05; - indicates no analysis results. ^a indicates wood density had a statistically significant impact at dowel diameter 10 mm and 0° loading. ^b indicates dowel diameter had a statistically significant impact with SPF

specimen under 0° loading. ° indicates loading angel had a statistically significant impact with Southern pine specimen and dowel diameter 12 mm.

3.2 Effect of thickness ratio of transverse layer

It is clear from Fig. 3 that CLT embedment strength decreased as TRTL increased. Furthermore, there was obvious difference of tested embedment strength value between normal CLT and GLT. For example, when loading under 0°, the embedment strength of GLT specimen, i.e. F-12-0.00-0, H-12-0.00-0 were 28% and 15% higher than those of normal CLT specimen, i.e. F-12-0.33-0, H-12-0.33-0, respectively. When loading under 90°, however, the embedment strength of GLT specimen, i.e. F-12-1.00-90, H-12-1.00-90 were 32% and 35% lower than those of normal CLT specimen, i.e. F-12-0.33-90, H-12-0.33-90, respectively. The reasons for these obvious differences were that normal CLT had orthotropic layup and that transverse and longitudinal layers bore the dowel embedment jointly. As it is known, the embedment strength of wood perpendicular to grain is much lower than that of wood parallel to grain and it is suggested to be only 44% of the embedment strength of wood parallel to grain in CSA O86 [13]. So TRTL plays an important effect on CLT embedment strength. Furthermore, TRTL also had statistically significant impact on CLT embedment strength, Table 5. Thus it could be drawn that these exiting design models for embedment strength of CLT should been modified based on CLT structural characteristics including TRTL.

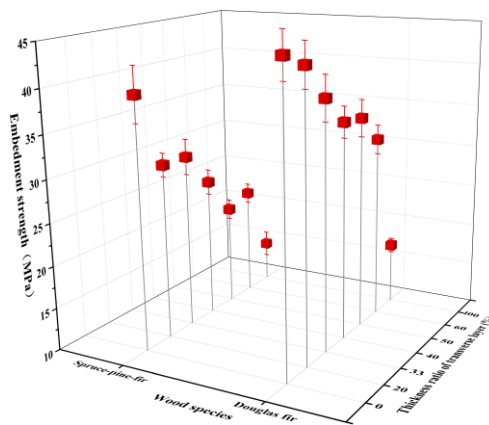


Fig. 3. Effect of TRTL on the embedment strength of CLT specimens with loading angle 0° and dowel diameter 12 mm

Table 5. Results of one-way analysis of variance of TRTL

| Wood species | | SS | DF | MS | F | Sig. |
|--------------|----------------|--------|-----|--------|-------|------|
| SPF | Between groups | 7311.8 | 6 | 1218.6 | 358.6 | 0.0 |
| | Within groups | 438.3 | 129 | 3.4 | | |
| | Total | 7750.2 | 135 | | | |
| Douglas fir | Between groups | 8881.3 | 6 | 1480.2 | | |
| | Within groups | 537.5 | 123 | 4.4 | 338.7 | 0.0 |
| | Total | 9418.8 | 129 | | | |

3.3 Evaluation of existing design equations

Although design models for embedment strength parallel and perpendicular-to-grain differ between codes, there has been general agreement about the Hankinson formula for the strength at any angle expressed as follows, Equation (2):

$$f_{\theta} = \frac{f_0 f_{90}}{f_0 \sin^2 \theta + f_{90} \cos^2 \theta} \quad (2)$$

where, f_0 = embedment strength parallel to grain; f_{90} = embedment strength perpendicular to grain; θ = angle of load to the grain of a layer.

All further discussion of the design models is built on the equations expressed in this format. The following notation is used in the equations presented in this section:

- $f_{\theta,avg}$ = average embedment strength (MPa);
- $f_{\theta,k}$ = characteristic embedment strength (MPa);
- d = fastener nominal diameter (mm);
- θ = loading angle relative to the specimen face layer grain (°);
- ρ_{12} = measured density based on volume and mass at 12% moisture content (g/cm^3);
- G_0 = measured relative density for the species or species group based on oven-dry mass and volume;
- G = mean relative density for the species or species group based on oven-dry mass and volume;
- and tt = thickness ratio of transverse layer.

To propose a design equation for CLT dowel embedment, the following models were considered in this study:

1. CLT embedment equations originating from the studies of Uibel and Balß;
2. CLT dowel embedment equation built in the studies of Kennedy et al;
3. The design model presented in the US edition of the CLT Handbook;
4. CSA O86 equation for CLT dowel embedment.

Individual experimental data were compared with the values predicted for the average embedment strength at 5-min. load duration. Then the experimental lower 5th percentile values based on 75% confidence obtained per series of approximate twenty replications were adjusted for the standard load duration (multiplied by 0.8 according to the CSA O86 Commentary [13]) and compared with design values predicted by the design equations (5th percentile values at standard load duration).

For design value, to convert the European model to the CSA O86 design values, the following adjustments are made:

1. Conversion from characteristic density at 12% moisture content to characteristic density at 15% moisture content (0.89);
2. Conversion from characteristic density at 15% moisture content to oven-dry characteristic density (relative density) (1.075);
3. Conversion from oven-dry characteristic density to mean relative density (0.8);
4. Conversion from short term to standard term (0.8) [8].

3.3.1 CLT embedment equations originating from the studies of Uibel and Balβ

Three design modes, independent of the build-up of CLT or not, were developed in the study of Uibel and Balβ, Equation (3), (4) and (5) [10,11].

$$f_{\theta,avg} = \frac{0.035(1-0.015d)\rho^{1.16}}{1.1\sin^2\theta + \cos^2\theta} \quad (3)$$

$$f_{\theta,avg} = 0.037(1-0.016d)\rho^{1.16} \left[\frac{\sum_{i=1}^n t_{0,i}}{t(1.2\sin^2\theta + \cos^2\theta)} + \frac{\sum_{j=1}^{n-1} t_{90,j}}{t(1.2\cos^2\theta + \sin^2\theta)} \right] \quad (4)$$

$$f_{\theta,k} = \frac{0.031(1-0.015d)\rho_k^{1.16}}{1.1\sin^2\theta + \cos^2\theta} \quad (5)$$

Where, t = total thickness of CLT; $t_{0,i}$ = thickness of individual longitudinal layer; $t_{90,i}$ = thickness of individual transverse layer.

3.3.2 CLT dowel embedment equation built in the studies of Kennedy et al;

The design models independent of dowel diameter and CLT panel layup were built by Kennedy et al. as shown in Equation (6) and (7) [6].

$$f_{\theta,avg} = \frac{80(\rho_{12} - 0.12)^{1.11}}{1.07(\rho_{12} - 0.12)^{-0.07} \sin^2\theta + \cos^2\theta} \quad (6)$$

$$f_{\theta,k} = \frac{41(\rho_{12} - 0.12)^{1.11}}{1.07(\rho_{12} - 0.12)^{-0.07} \sin^2\theta + \cos^2\theta} \quad (7)$$

3.3.3 The design model presented in the US edition of the CLT Handbook

The layup characteristics of CLT were considered in the design model presented in the US edition of the CLT Handbook. According to this design model, the embedment strength of the face layer is associated with the “effective” bearing length of the fastener, which is adjusted in proportion between the embedment strengths of the cross layer and the parallel layer [1,6]. If applied directly to the embedment strength of CLT, this model can be expressed as Equation (8) [1].

$$f_{\theta,CLT} = (l_{//}f_{\theta} + l_{\perp}f_{90-\theta})l_p^{-1} \quad (8)$$

Where, $l_{//}$ = fastener bearing length in parallel layer(s); l_{\perp} = fastener bearing length in cross layer(s); l_p = total bearing length of fastener in CLT panel; f_{θ} = embedment strength of parallel layer(s); and $f_{90-\theta}$ = embedment strength of cross layer(s).

The average and design values equations for embedment strength of individual layer parallel and perpendicular to grain are expressed as Equation (9) and (10) [1].

$$f_{0,avg} = 77G_0 \quad f_{90,avg} = 212G_0^{1.45}d^{-0.5} \quad (9)$$

$$f_{0,k} = 44G \quad f_{90,k} = 105G^{1.45}d^{-0.5} \quad (10)$$

3.3.4 CSA O86 equation for CLT dowel embedment

In this model, the only difference of embedment strength design model for CLT is that the embedment strength of parallel layer is multiplied by 0.9 based on the value of wood or wood products. Hence the average and design values equations at any loading angle for CLT are expressed as Equation (11) and (12), respectively [13].

$$f_{\theta,avg} = \frac{0.9 \times 82 \rho_{12} (1 - 0.01d)}{0.9 \times 2.27 \sin^2\theta + \cos^2\theta} \quad (11)$$

$$f_{\theta,k} = \frac{0.9 \times 50G(1 - 0.01d)}{0.9 \times 2.27 \sin^2\theta + \cos^2\theta} \quad (12)$$

Non-linear regression analysis was performed for the average values calculated by existing design models. Several statistical parameters were estimated for predicting average values of each equation [15], Table 6. It tends to overestimate predictions for all equations and the Equation (8) and (9) presented in the US edition of the CLT Handbook behaves better than other equations. However, as for the pseudo R², all of the equations are low and the Equation (3) and Equation (4) show questionable fit. The statistic results indicate these existing models should be improved.

Table 6 Statistical comparison of existing design models

| Equation | RMSE | MAE | APE | Pseudo R ² |
|----------|------|------|--------|-----------------------|
| (3)* | 9.22 | 7.80 | 27.66% | -28.21% |
| (4)* | 9.03 | 7.62 | 27.19% | -22.89 % |
| (6) | 8.20 | 6.62 | 20.58% | 14.32% |
| (8,9) | 6.51 | 4.90 | 18.03% | 45.92% |
| (11) | 8.16 | 6.30 | 19.86% | 15.22% |

Where, * indicates the test data used to evaluate this model meet the equation requirement, i.e. the ratio of sum of layer thicknesses oriented parallel to outer layers and the sum of layer thicknesses oriented perpendicular to outer layers was between 0.95 and 2.1.

3.4 New CLT dowel embedment equation

Based on the above results of analysis of variance, nonlinear regression analyses were performed by Matlab software to develop an equation for the CLT dowel embedment strength dependent of wood density, dowel diameter, loading angle, and TRTL of CLT, Equation (13) and (14).

$$f_{\theta,avg} = 0.3364(0.4541 - 0.0205d)\rho_{12} \left(\frac{tt}{1.4101\cos^2\theta + \sin^2\theta} + \frac{1-tt}{1.4101\sin^2\theta + \cos^2\theta} \right) \quad (13)$$

$$f_{\theta,k} = 0.2575(0.4541 - 0.0205d)\rho_{12} \left(\frac{tt}{1.4101\cos^2\theta + \sin^2\theta} + \frac{1-tt}{1.4101\sin^2\theta + \cos^2\theta} \right) \quad (14)$$

Where, tt = thickness ratio of transverse layer of CLT, $0 \leq tt \leq 1$.

All the tested CLT specimens only have three layers and the adjacent layers were orthogonally arranged in this study. It is possible that the layer number and other layer orientation, such as two adjacent outer layers

oriented parallel to each other [5], also affect the embedment strength of CLT which may be studied in later period. So the validity of Equation (13) and (14) is limited to three-layer CLT with adjacent layers orthogonally arranged. By the way, when $t=0$ or 1, Equation (13) and (14) could be used to calculate the embedment strength of GLT parallel or perpendicular to grain, respectively.

Fig. 4 and Fig. 5 shows the comparison between predicted average and design values calculated by Equation (13) and (14) and test values, respectively.

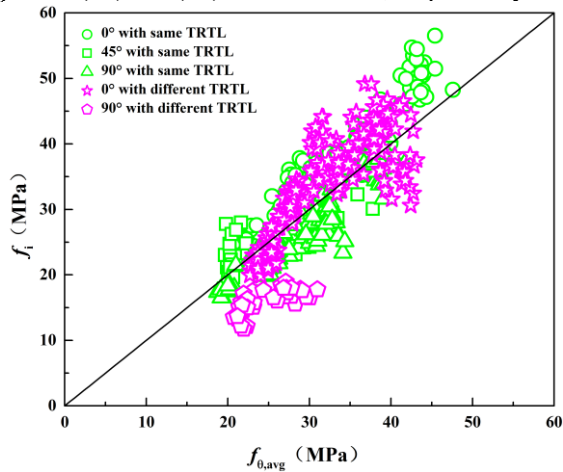


Fig. 4. Comparison of Equation (13) vs. test data

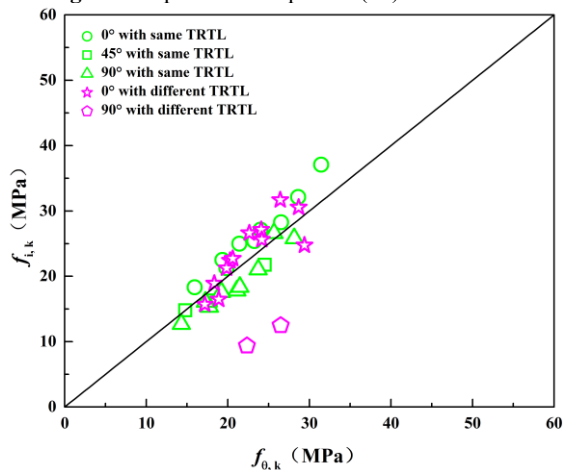


Fig. 5. Comparison of Equation (14) vs. test data adjusted to standard load duration

This new model provides fair predictions for the average embedment strength. As shown in Fig.4, predictions present a better fit with the experimental values for all test data. Indeed, Equation (13) shows the best pseudo R^2 values from the non-linear analysis in comparison with other design models considered. Even though this equation tends to slightly over-predict the strength, it generally performs well with the following statistical results, Table 7.

Table 7 Statistical comparison of new design model

| Design method | RMSE | MAE | APE | Pseudo R^2 |
|---------------|------|------|--------|--------------|
| Equation (13) | 4.72 | 3.83 | 13.29% | 71.58% |

4 Load-displacement behaviour and failure mode

Respective load-displacement behaviours of CLT specimens under 0° , 45° and 90° loading are shown in Fig. 6. All load-displacement behaviours were linear in initial stage. The test specimens under 0° loading had best elastic properties, then was 45° and 90° specimens. Brittle failures were observed in the 45° specimens, however, the 0° and 90° specimens still experienced significant ductile deformation. On the other hand, no significant differences of load-displacement behaviour were observed in the specimens with various wood species and dowel diameter, Fig. 6.

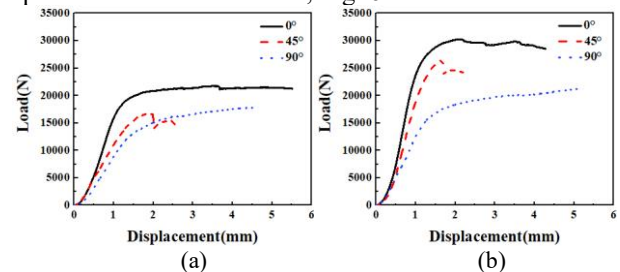


Fig. 6. Load-displacement behaviour of CLT specimens (a) SPF CLT, and (b) Southern pine CLT

Fig. 7 presents the respective embedment load-displacement curves of CLT and GLT tested under same dowel embedment conditions. It was obvious that the deformation under 0° loading of CLT and GLT were ductile and brittle, respectively, Fig. 7(a). Similar discovery was obtained in [3]. This ductile behaviour of CLT is due to the orthogonal layup where transverse layers act as reinforcement and prevent early failures in tension perpendicular to grain and block or row shear [3]. However, there was not obvious differences of load-displacement curve between CLT and GLT under 90° loading due to most of transverse layers bearing the embedment, Fig. 7(b).

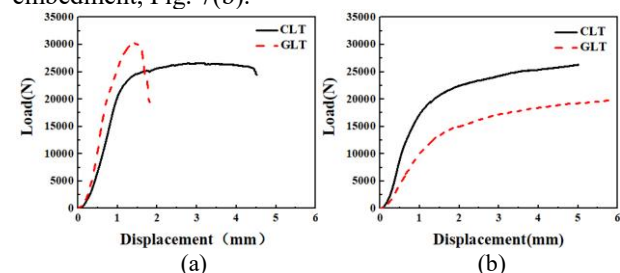


Fig. 7. Load-displacement behaviour of Douglas fir CLT and GLT, (a) 0° loading and (b) 90° loading

As for failure modes, the respective failure modes of specimen(s) tested under various loading angle are shown in Fig. 8. The main failure mode of specimens under 0° loading was crack occurring along grain in the middle of outer layer (longitudinal layer) and compression failure in the top of core layer (transverse layer), Fig. 8(a). When loading under 45° , the main failure mode of specimens was crack occurring along the grain of outer layer, Fig. 8(b). However, the main failure mode of specimens under 90° loading was compression failure in the top of outer layer and delamination of the bondline between outer and core layer, Fig. 8(c). No obvious differences of failure modes of specimens with

various wood species and dowel diameters were observed in this study.

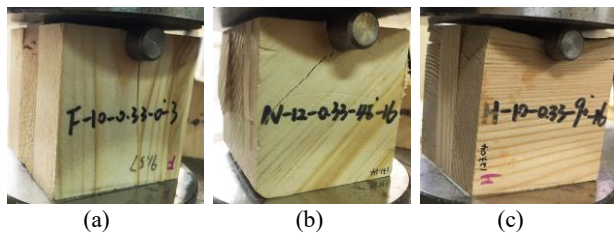


Fig. 8. Failure modes under various loading angle, (a) 0°, (b) 45° and (c) 90°

5 Conclusions

This study focused on the impacts of wood density, smooth dowel diameter, loading angle, and the especial layup feature of CLT, i.e. the thickness ratio of transverse layer (TRTL) on CLT embedment strength.

The direct-viewing analysis of test data showed different factors had different influence tendency on CLT embedment strength. For example, CLT embedment strength increased as wood density increased, however, it decreased as dowel diameter, loading angle or TRTL increased. Furthermore, the one-way analysis of variance results showed each factor had statistically significant impact on CLT embedment strength.

A few of existing design models (Uibel and Blaß, Kennedy et al, US edition of the CLT Handbook and CSA O86) for CLT embedment strength were evaluated using the experimental data. Based on the results of statistical comparison between equations and one-way analysis of variance, a new approach, dependent of the wood density, smooth dowel diameter, loading angle and TRTL was developed in this study. The results of statistical comparison showed this new approach behaved better than other equations.

Finally, the load-displacement behaviour and failure modes of CLT under dowel embedment were analyzed. The specimens tested under different loading angles had obviously different failure modes. There were obvious differences between embedment behaviour under 0° loading and embedment strength between CLT and GLT.

References

1. E. Karacabeyli, B. Douglas, *CLT handbook: cross-laminated timber, U.S. Ed.* (FPInnovations, Quebec, 2013).
2. C. Silva, J.M. Branco, A. Ringhofer, P.B. Lourenço, G. Schickhofer, *Constr. Build. Mater.* **125**, 1205 (2016)
3. A. Ringhofer, R. Brandner, H.J. Blaß, *Eng. Struct.* **171**, 849 (2018)
4. Z. Wang, J. Zhou, W. Dong, Y. Yao, M. Gong, *Maderas-Cienc. Tecnol.* **20** (3), 469 (2018)
5. *EN 16351:2015, Timber structures–Cross laminated timber–Requirements* (CEN, Brussels, 2015)
6. S. Kennedy, A. Salenikovich, W. Munoz, M. Mohammad, *Proceedings of the World Conference on Timber Engineering* (2014)
7. C.L. Santos, A.M.P.D. Jesus, J.J.L. Morais, J.L.P.C. Lousada, *Strain* **46** (2), 159 (2010)
8. S. Kennedy, A. Salenikovich, W. Munoz, M. Mohammad, D. Sattler, *Proceedings of the World Conference on Timber Engineering* (2014).
9. D. Zhou, D. Guan, *Prog. Struct. Eng. Mater.* **8** (2), 49 (2006)
10. T. Uibel, H.J. Blaß, *39th CIB-W18 Meeting*, Paper 39-7-5 (2006)
11. T. Uibel, H.J. Blaß, *COST Action FP1004, Focus Solid Timber Solutions–European Conference on Cross Laminated Timber (CLT)*, pp. 119–134 (2013)
12. T. Uibel, H.J. Blaß, *Proceedings of the 44th CIB-W18 meeting*, Paper 40-7-2 (2007)
13. *CSA O86-14, Engineering design in wood*, (CSA Group, Mississauga, 2014)
14. K. Sawata, M. Yasumura, *J. Wood Sci.* **48** (2), 138 (2002)
15. S. Kennedy, *Withdrawal and embedding resistance of fasteners in timber and CLT panels* (Laval University, Quebec, 2014)